Hydrothermal Stability and Catalytic Activity of Aluminum-Containing Mesoporous Ethane−Silicas

Qihua Yang,* Ying Li, Lei Zhang, Jie Yang, Jian Liu, and Can Li

State Key Laboratory of Catalysis, Dalian Institute of Chemical Physics, Chinese Academy of Sciences, Dalian, 116023, China

Received: February 10, 2004

Aluminum was incorporated into the mesoporous framework of ethane−silica by one-pot condensation of $Al(OiPr)_3$ with 1,2-bis(trimethoxysilyl)ethane using octadecyltrimethylammonium chloride as surfactant. Powder X-ray diffraction patterns, nitrogen sorption analysis, and TEM results reveal the formation of an ordered mesoporous material with uniform porosity. ^{27}Al MAS NMR confirms the incorporation of aluminum in the framework. The synthesized materials exhibit extremely high hydrothermal stability in boiling water (no obvious change of mesostructure and textural properties was observed even after refluxing in water for 100 h), which could be mainly contributed to the ethane-bridged mesoporous framework. The aluminum-containing mesoporous ethane−silicas are efficient catalysts for the alkylation of 2,4-di-*tert*-butylphenol by cinnamyl alcohol to yield a flavan.

Introduction

Recently, the periodic mesoporous organosilicas (PMOs) synthesized from organosilanes, $(RO)_3Si-R-Si(OR)_3$, have attracted much research attention.[1−5] The PMOs with organic group bridged in the framework have advantages compared with the SiO_2-based mesoporous materials, such as the tunable surface hydrophobicity/hydrophilicity, modified mechanical stability, and the homogeneously distributed organic group in the framework.[6] The unique catalytic property could be expected from the PMOs with the merits mentioned above. For its application in the field of catalysis, the incorporation of metal active sites into the channel wall of PMOs is very important.[7]

Microporous aluminosilicate molecular sieves are very useful heterogeneous catalyst, but their small pore size is not suitable for processing large molecules. The mesostructured MCM-41 offers the possibility to deal with molecules in the mesoporous range (2−50 nm). Incorporation of Al in the MCM-41 framework is of great interest for the petrochemical industry and manufacture of fine chemicals and pharmaceuticals, but the low hydrothermal stability of Al−MCM-41 limits its wide applications. Great efforts have been made to improve the hydrothermal stability of Al-containing mesoporous materials, such as postsynthesis grafting, synthesis of mesoporous materials with thick pore walls, synthesis of mesoporous materials with semicrystalline walls, preparing mesoporous aluminosilicates from performed zeolite nanoclusters, generating microporous zeolite-mesostructure, and synthesis of ultrastable mesoporous materials at high temperature.[8−14] However, the synthesis of Al-containing mesoporous material with high hydrothermal stability remains a big challenge. Previous studies show PMOs exhibit extremely high stability in boiling water.[1,15] Introducing Al into the framework of mesoporous ethane−silica may not only result in material with high hydrothermal stability but can also expand the application fields of PMOs. In this work we report the incorporation of Al into the framework of mesoporous ethane−silica (MES−Al). The synthesized MES−Al exhibits hydrothermal ultrastability in boiling water (no obvious change of mesostructure and textural properties was observed even after refluxing in water for 100 h), which could be mainly contributed to the hydrophobic ethane-bridged mesoporous framework. The catalytic properties of the materials were investigated by choosing the alkylation of 2,4-di-*tert*-butylphenol with cinnamyl alcohol as model reaction.

Experimental Section

Materials. All materials were analytical grade and used as purchased without further purification. 1,2-Bis(trimethoxysilyl)-ethane (BTME), octadecyltrimethylammonium chloride (C_{18}-TMACl), and aluminum isopropoxide ($Al(OiPr)_3$) were purchased from Sigma-Aldrich Co. Ltd.

Synthesis of the Materials. The typical synthesis procedure for aluminum-incorporated mesoporous ethane−silica was as follows: C_{18}TMACl (1.20 g) was dissolved in deionized water (38.00 g), followed by addition of NaOH (0.57 g). BTME (1.62 g) was poured into the above mixture, the solution was stirred at room temperature for 20 min, and then desired amount of $Al(OiPr)_3$ was added as a solid in small portions (0.06 and 0.12 g for MES−Al-1 and MES−Al-2, respectively). Finally, the mixture was further stirred at ambient temperature for an additional 12 h and aged under reflux at 98 °C for another 24 h. The white precipitate was filtered, repeatedly washed with deionized water, and dried. The sample was denoted as MES−Al. The Si/Al ratio in the initial mixture was 40/1 and 20/1 for MES−Al-1 and MES−Al-2, respectively. The surfactant was removed by solvent extraction using an HCl−ethanol solution.[1] To investigate the hydrothermal stability of the material, the sample was subjected to refluxing in deionized water (with 1 L of water per gram of solid) for 48−100 h. After refluxing, the sample was filtered and dried.

Catalytic Experiment. The alkylation of 2,4-di-*tert*-butylphenol with cinnamyl alcohol was performed in a 50 mL flask. A mixture of 0.25 mmol of 2,4-di-*tert*-butylphenol (Aldrich),

* Corresponding author. Tel: 86-411-4379552. Fax: 86-411-4694447. E-mail: yangqh@dicp.ac.cn.

10.1021/jp040124o CCC: $27.50
Published on Web 05/07/2004

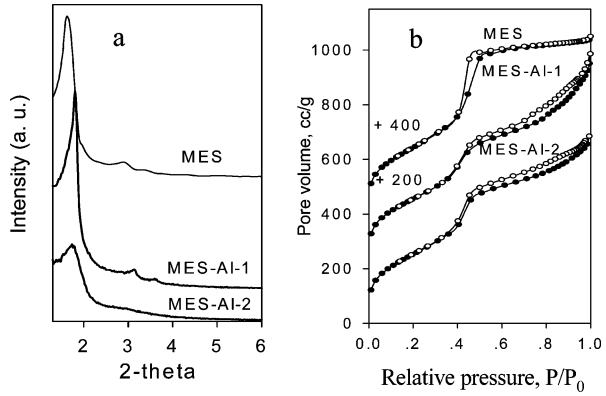

Figure 1. XRD patterns (a) and nitrogen isotherms of MES−Al.

0.25 mmol of cinnamyl alcohol (Aldrich), 125 mg of catalyst in 12.5 mL of isooctane was stirred at 95 °C for 24 h. After the reaction, the mixture was filtered and the filtrate was analyzed on an Agilent 6890 gas chromatograph equipped with a flame ionization detector and an OV-1 capillary column (30 m × 0.25 mm × 0.3 μm) using 1,3-di-*tert*-butylbenzene as an internal standard.

Characterization. X-ray powder diffraction (XRD) patterns were recorded on a Rigaku D/Max 3400 powder diffraction system using Cu Kα radiation. The nitrogen sorption experiments were performed at 77 K on an ASAP 2000 system, and the samples were outgassed at 100 °C for 10 h before the measurement. Pore diameters were determined from adsorption branches using the Barretl−Joyner−Hulenda (BJH) method. High-resolution transmission electron microscopy (TEM) was performed using a JEM-2010 at an acceleration voltage of 200 kV. ^{27}Al, ^{13}C, and ^{29}Si MAS NMR spectra were recorded in a 4-mm ZrO_2 rotor on a Bruker DRX-400 spectrometer equipped with a magic angle spin probe. ^{27}Al signals were referenced to a 0.5 M aqueous solution of aluminum nitrate. ^{13}C and ^{29}Si signals were referenced to tetramethylsilane (TMS).

Acidity by Pyridine Adsorption Using FT-IR. Infrared spectra were recorded on a Thermo Nicolet Nexus 470 FT-IR spectrometer. Self-supporting wafers of 1.3 cm were loaded into an IR cell with CaF_2 windows. The wafer was degassed at 250 °C for 2 h under a vacuum of 10^{-1} Pa before the introduction of pyridine. FT-IR spectra of adsorbed pyridine were recorded at room temperature after evacuating the cell and desorption of the weakly adsorbed pyridine at 150 °C

Results and Discussion

Mesostructure and Porosity of the Materials. Powder X-ray diffraction spectra of surfactant-free MES−Al exhibits narrow (100) peaks and, in most cases, well-separated (110) and (200) reflections, indicating that the samples have hexagonal structure with a high degree of structural ordering (Figure 1a).[16] Compared with MES, the decreasing of d_{100} spacing of MES−Al evidences the lattice contraction during Al incorporation. The structural order of the sample with less Al incorporation is almost the same as that of mesoporous ethane−silica (MES), while with more Al incorporation, the intensity of the (100) peak decreases and also the higher order peaks disappear. This result illustrates that the long-range structural order is disturbed with Al incorporation.

The nitrogen adsorption/desorption isotherms of surfactant-free MES−Al are of type IV with a nitrogen condensation step characteristic of mesoporous materials with narrow pore size distributions (Figure 1b). The TEM images of MES−Al-1 clearly show the hexagonal arrangement of uniform channels

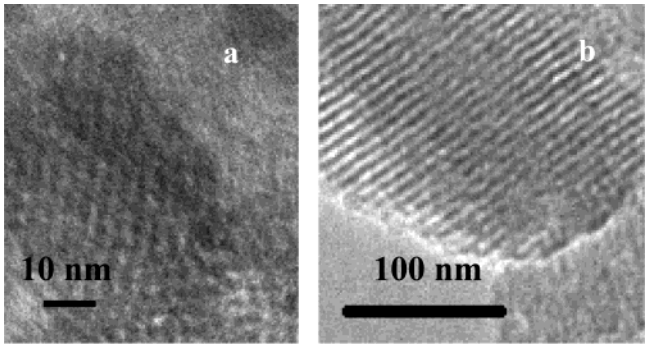

Figure 2. TEM images of MES−Al-1 (a) in the direction of the pore axis and (b) in the direction perpendicular to the pore axis.

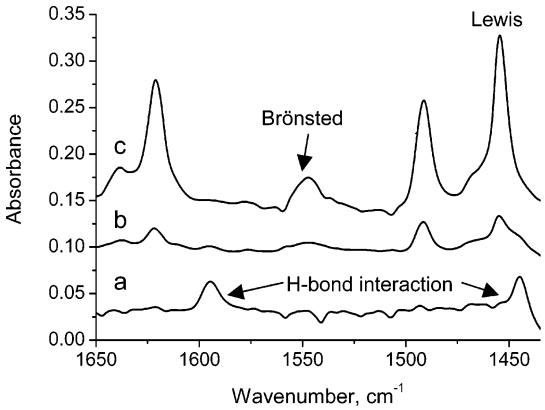

Figure 3. FT-IR spectra of the adsorbed pyridine after pyridine adsorption and then desorption at 150 °C: (a) MES, (b) MES−Al-1, (c) MES−Al-2.

(Figure 2). The mesopore filling step for MES−Al shifts to relatively lower pressure in comparison with pure MES, displaying the lattice contraction as also observed by XRD. An obvious hysteresis at $P/P_0 > 0.45$ is observed for MES−Al, which could be attributed to the existence of interparticle pores.[17,18] MES shows much higher and steeper capillary condensation step than MES−Al, indicating that the ordered mesoporous structure is disturbed by aluminum incorporation, which is consistent with XRD results.

Compositional Information of the Materials. The FT-IR spectra of pyridine adsorption on MES−Al samples (Figure 3) show two intense bands at 1547 and 1455 cm^{-1}, which are characteristic of Brönsted and Lewis acid sites, respectively.[19] Almost no acidity is observed for MES material without Al (the bands at 1445 and 1594 cm^{-1} are probably due to the pyridine adsorbed via H-bond interaction). Thus, the result of pyridine adsorption proves that Al is incorporated in the ethane-bridged mesoporous framework.

The compositional information of MES−Al was investigated using a solid NMR technique. The ^{27}Al MAS NMR spectrum of MES−Al-1 (Si/Al = 54) exhibits its main resonance at 55 ppm, which is characteristic of tetrahedral aluminum centers (Figure 4a). This indicates that most of aluminum is incorporated into the mesoporous framework. For MES−Al-2 with a Si/Al ratio of 29, two resonances are observed at 55 ppm (tetrahedral aluminum center) and 0 ppm (octahedral aluminum center). This implies the formation of both framework and extraframework aluminum center for samples with higher aluminum concentration. ^{29}Si MAS NMR shows two signals at −59.1 and −66.7 ppm, which could be assigned to the T^2 and T^3 site of silicon species bonded with ethane group, respectively (Figure 4b). It was reported that T^2 site [*Si*COH(OSi)$_2$] of MES was found at −57.0 ppm.[1] The shift of the T^2 site of MES−Al-2 upfield is

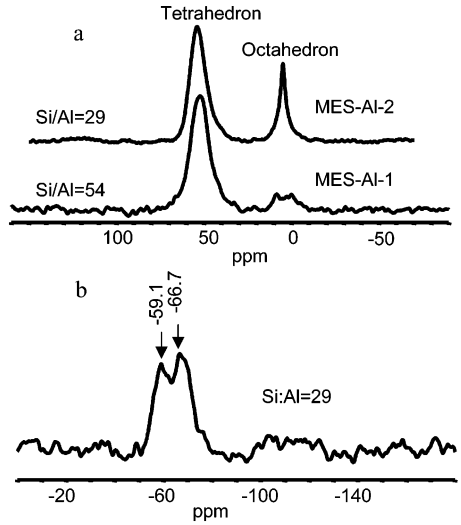

Figure 4. ^{27}Al (a) and ^{29}Si (b) MAS NMR spectra of surfactant-free MES−Al.

due to the formation of *Si*C(OAl)(OSi)$_2$ species,[20] which further confirms the Al incorporation in the mesoporous framework. The ^{13}C CP MAS NMR spectrum of surfactant-free MES−Al-2 gives the signal for the ethane fragment at 5.4 ppm, indicating no Si−C bond cleavages during the synthesis.[1] The NMR results show that the aluminum is successfully incorporated in ethane-bridged framework and the Si−C bond remains intact during the synthesis process.

Hydrothermal Stabilities of MES−Al. Previous studies of mesoporous ethane−silica show that no collapse of mesoporous structure was observed after the material was refluxed in boiling water for 8 h.[1] The hydrothermal stability of mesoporous ethane−silica is attributed to the hydrophobic ethane-bridged framework. During our investigations of PMOs, we found the mesoporous ethane−silica was stable in boiling water for more than 100 h (see Supporting Information). The hydrothermal stability of aluminum-incorporated mesoporous ethane−silica was also investigated. The hexagonal mesostructure of MES−Al-*n* (n = 1, 2) after treatment (refluxing in boiling water for 100 h) is well-defined as noted in most cases by (100), (110), and (200) peaks (Figure 5a). The nitrogen adsorption/desorption isotherms of MES−Al-*n* (n = 1, 2) after the treatment resemble that of the untreated ones, implying that the textural properties are almost the same before and after the treatment in boiling water (Figure 5b, Table 1). Interestingly, unlike MES, the BET surface area of MES−Al-*n* (n = 1, 2) is slightly increased after the treatment (Table 1). This may be due to the transfer of big pore to mesopore after the treatment of MES−Al-*n* (n = 1, 2). The results of XRD and nitrogen isotherms demonstrate that the MES−Al-*n* (n = 1, 2) exhibit quite high hydrothermal stability in boiling water. The hydrothermal ultrastability of MES−Al-*n* (n = 1, 2) could be mainly attributed to the hydrophobic ethane−bridged framework.

TABLE 1: Elemental Composition and Textural Properties of Surfactant-Free MES−Al before and after Hydrothermal Treatment

sample	Si/Al[a]	surface area ($m^2\ g^{-1}$)	pore volume ($cm^2\ g^{-1}$)	pore diameter (nm)[b]	wall thickness (nm)[c]
MES		912	0.98	3.58	2.69
refluxed 48 h		853	0.81	3.30	2.63
refluxed 100 h		847	0.78	3.34	2.85
MES-Al-1	54	939	1.01	3.48	2.18
refluxed 48 h	52	1072	1.22	3.51	2.47
refluxed 100 h	52	1088	1.20	3.42	2.10
MES-Al-2	29	941	1.12	3.43	2.43
refluxed 48 h	28	988	1.21	3.37	2.63
refluxed 100 h	26	972	1.21	3.40	2.46

[a] Calculated from elemental analysis. [b] Calculated from adsorption branch. [c] Calculated by a_0 − pore size, where $a_0 = 2d_{100}/\sqrt{3}$.

Catalytic Properties of MES−Al. The alkylation of 2,4-di-*tert*-butylphenol by cinnamyl alcohol to yield a flavan was chosen as model reaction to evaluate the textural mesoporosity and catalytic properties of aluminum-containing mesoporous ethane−silica, because the yield and selectivity to flavan is an indicator of the effectiveness of the moderately acidic sites in the mesoporous framework. MES−Al-*n* (n = 1, 2) are efficient catalysts for the alkylation reaction (Table 2). Two types of main product were observed on MES−Al catalysts, product **1** (primary cinnamylphenol) and product **2** (dihydrobezebbenzopyran-flavan). Product **2** is formed through the intramolecular ring closure of the product 1.[21] Higher conversion of 2,4-di-*tert*-butylphenol on Al-MES catalyst was observed than that on Al−MCM-41.[22] The higher activity of MES−Al could be probably attributed to the fact that the hydrophobic ethane-bridged framework makes an easy access of reactants to the Al active site. However, flavan yield on Al-MES catalysts is much lower than that on Al−MCM-41, this might be due to the weak acidity of the aluminum active site in Al-MES catalyst. With aluminum concentration increasing, both the conversion of 2,4-di-*tert*-butylphenol and the selectivity to flavan increased. The catalytic activity and selectivity of MES−Al-2 after hydrothermal treatment were also investigated. After hydrothermal treatment, the material still exhibits high catalytic activity. This result further confirms the structural and compositional stability

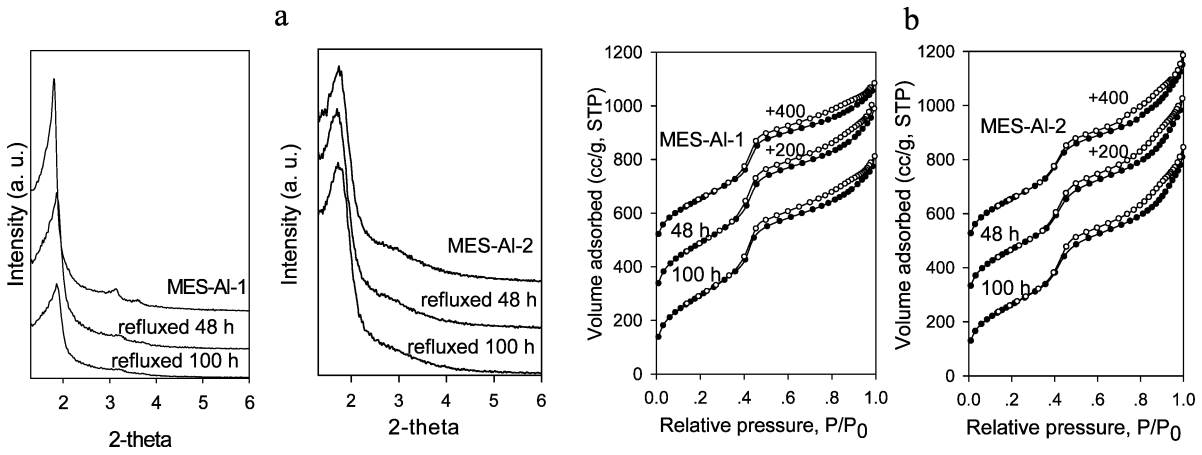

Figure 5. XRD patterns (a) and nitrogen isotherms (b) of surfactant-free MES−Al before and after refluxing in water.

TABLE 2: Alkylation of 2,4-Di-*tert*-butylphenol with Cinnamyl Alcohol in the Presence of MES−AL[a]

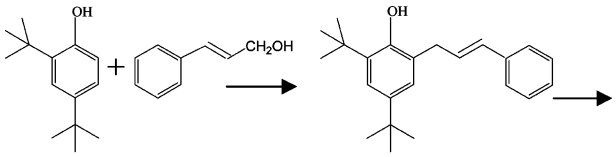

Product 1

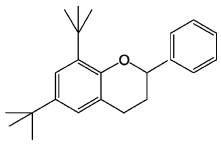

Product 2-flavan

catalyst	conversion (%)	selectivity (mol %)		flavan yield (%)
		1	**2**	
MES-Al-1	59.3	61.9	11.7	6.9
MES-Al-2	70.4	47.6	25.3	17.8
MES-Al-2-48	62.3	57.1	11.3	7.0
MES-Al-2-100	70.8	48.1	6.6	4.7
Al-MCM-41[22]	47.2		71.8	33.9

[a] Reaction conditions: 2,4-di-*tert*-butylphenol (0.25 mmol), cinnamyl alcohol (0.25 mmol), catalyst (125 mg), isooctane (12.5 mL), 95 °C, 24 h.

of MES−Al in boiling water. Longer refluxing time of MES−Al-2 leads to lower total flavan yield. The FT-IR spectra of pyridine adsorption on MES−Al-2−100 samples (see Supporting Information) show only one intense band at 1455 cm^{-1} (Lewis acid sites). The disappearance of Brönsted acid sites on MES−Al-2−100 indicates that the acidity of MES−Al-2 decreased after hydrothermal treatment. The above results indicate that the surrounding environment of aluminum species changed somewhat after hydrothermal treatment.

Conclusion

Aluminum-incorporated mesoporous ethane−silica with hydrothermal ultrastability can be synthesized by one-pot condensation of BTME and $Al(OiPr)_3$. The novel hydrothermally ultrastable materials having both hydrophobic and acidic functionality promise to attract much attention in the wide fields of chemistry, especially in the field of acid/base catalysis. The hydrophobic ethane-bridged framework is one of the main reasons for the hydrothermal stability of MES−Al, and the synthesis of PMOs with heteroatom in the framework provides a new approach for obtaining hydrothermally stable mesoporous material with new properties.

Acknowledgment. This work was financially supported by the National Science Foundation of China (20303020), the National Basic Research Program of China (2003CB615803), and the Talent Science Program of the Chinese Academy of Sciences.

Supporting Information Available: Powder X-ray diffraction patterns and nitrogen isotherms of mesoporous ethane−silica before and after hydrothermal treatment; FT-IR spectra of pyridine adsorption on MES−Al-2−100. This material is available free of charge via the Internet at http://pubs.acs.org.

References and Notes

(1) Inagaki, S.; Guan, S.; Fukushima, Y.; Ohsuna, T.; Terasaki, O. *J. Am. Chem. Soc.* **1999**, *121*, 9611.
(2) Melde, B. J.; Holland, B. T.; Blanford, C. F.; Stein, A. *Chem. Mater.* **1999**, *11*, 3302.
(3) Asefa, T.; MacLachlan, M. J.; Coombs, N.; Ozin, G. A. *Nature* **1999**, *402*, 867.
(4) Guan, S.; Inagaki, S.; Ohsuna, T.; Teresaki, O. *J. Am. Chem. Soc.* **2000**, *122*, 5660.
(5) Inagaki, S.; Guan, S.; Ohsuna, T.; Terasaki, O. *Nature* **2002**, *416*, 304.
(6) Yoshina-Ishii, C.; Asefa, T.; Coombs, N.; MacLachlan, M. J.; Ozin, G. A. *Chem. Commun.* **1999**, 2539.
(7) (a) Kapoor, M. P.; Sinha, A. K.; Seelan, S.; Inagaki, S.; Tsubota, S.; Yoshida, H.; Haruta, M. *Chem. Commun.* **2002**, 2902. (b) Park, S. S.; Cheon, J. H.; Park, D. H. *Stud. Surf. Sci. Catal.* **2003**, *146*, 481.
(8) Mokaya, R. *Angew. Chem., Int. Ed. Engl.* **1999**, *38*, 2930.
(9) Kim, S. S.; Zhang, W. Z.; Pinnavaia, T. J. *Science* **1998**, *282*, 1302.
(10) On, D. T.; Kaliaguine, S. *Angew. Chem., Int. Ed.* **2001**, *40*, 3248.
(11) Zhang, Z.; Han, Y.; Xiao, F. S.; Qiu, S.; Zhu, L.; Wang, R.; Yu, Y.; Zhang, Z.; Zou, B.; Wang, Y.; Sun, H.; Zhao, D.; Wei, Y. *J. Am. Chem. Soc.* **2001**, *123*, 5014.
(12) Zhang, Z.; Han, Y.; Zhu, L.; Yang, R.; Yu, Y.; Qiu, S.; Zhao, D.; Xiao, F. S. *Angew. Chem., Int. Ed.* **2001**, *40*, 1258.
(13) (a) On, D. T.; Kaliaguine, S. *Angew. Chem., Int. Ed.* **2002**, *41*, 1036. (b) Liu, Y.; Zhang, W.; Pinnavaia, T. J. *J. Am. Chem. Soc.* **2000**, *122*, 8791.
(14) Han, Y.; Li, D.; Zhao, L.; Song, J.; Yang, X.; Li, N.; Di, Y.; Li, C.; Wu, S.; Xu, X.; Meng, X.; Lin, K.; Xiao, F. S. *Angew. Chem., Int. Ed.* **2003**, *42*, 3633.
(15) Burleigh, M. C.; Markowitz, M. A.; Jayasundera, S.; Spector, M. S.; Thomas, C. W.; Gaber, B. P. *J. Phys. Chem. B* **2003**, *107*, 12628.
(16) Kresge, C. T.; Leonowicz, M. E.; Roth, W. J.; Vartuli, J. C.; Beck, J. S. *Nature* **1992**, *359*, 710.
(17) Kruk, M.; Jaroniec, M.; Sakamoto, Y.; Terasaki, O.; Ryoo, R.; Ko, C. H. *J. Phys. Chem. B* **2000**, *104*, 292.
(18) (a) Alfredsson, V.; Keung, M.; Monnier, A.; Stucky, G. D.; Unger, K.; Schuth, F. *J. Am. Chem. Soc., Chem. Commun.* **1994**, 921. (b) Chenite, A.; Le Page, Y.; Sayari, A. *Chem. Mater.* **1995**, *7*, 1015.
(19) Liu, Y.; Pinnavaia, T. J. *J. Mater. Chem.* **2002**, *12*, 3179.
(20) Lindner, E.; Jäger, A.; Auer, F.; Wegner, P.; Mayer, H. A.; Benzen, A.; Adam, D.; Plies, E. *Chem. Mater.* **1998**, *10*, 217.
(21) Armengol, E.; Cano, M. L.; Corma, A.; Garcia, H.; Navarro, M. T. *J. Am. Chem. Soc., Chem. Commun.* **1995**, 519.
(22) Pauly, T. R.; Liu, Y.; Pinnavaia, T. J.; Billinge S. J. L.; Rieker, T. P. *J. Am. Chem. Soc.* **1999**, *121*, 8835.